



Large contribution of fossil fuel derived secondary organic carbon to water soluble organic aerosols in winter haze in China

Yan-Lin Zhang^{1,2,3,6}, Imad El-Haddad³, Ru-Jin Huang^{3,4}, Kin-Fai Ho^{4,5}, Jun-Ji Cao⁴, Yongming Han⁴, Peter Zotter³, Carlo Bozzetti³, Kaspar R. Daellenbach³, Jay G. Slowik³, Gary Salazar², André S. H. Prévôt³, and Sönke Szidat²

¹Yale-NUIST Center on Atmospheric Environment, Nanjing University of Information Science and Technology, 210044 Nanjing, China

²Department of Chemistry and Biochemistry & Oeschger Centre for Climate Change Research, University of Bern, 3012 Bern, Switzerland

³Paul Scherrer Institute (PSI), 5232 Villigen, Switzerland

⁴Key Laboratory of Aerosol Chemistry and Physics, Institute of Earth Environment, Chinese Academy of Sciences, 710061 Xi'an China

⁵School of Public Health and Primary Care, The Chinese University of Hong Kong, Hong Kong, China

⁶Key Laboratory of Meteorological Disaster, Ministry of Education (KLME)/Collaborative Innovation Center on Forecast and Evaluation of Meteorological Disasters (CIC-FEMD), Nanjing University of Information Science & Technology, Nanjing 210044, China

Correspondence: Yan-Lin Zhang (dryanlinzhang@outlook.com, zhangyanlin@nuist.edu.cn), André S. H. Prévôt (andre.prevot@psi.ch), Ru-Jin Huang (rujin.huang@ieecas.cn), Jun-Ji Cao (jjcao@ieecas.cn) and Sönke Szidat (szidat@dcb.unibe.ch)

Received: 6 December 2017 – Discussion started: 12 December 2017

Revised: 16 February 2018 – Accepted: 19 February 2018 – Published: 22 March 2018

Abstract. Water-soluble organic carbon (WSOC) is a large fraction of organic aerosols (OA) globally and has significant impacts on climate and human health. The sources of WSOC remain very uncertain in polluted regions. Here we present a quantitative source apportionment of WSOC, isolated from aerosols in China using radiocarbon (¹⁴C) and offline high-resolution time-of-flight aerosol mass spectrometer measurements. Fossil emissions on average accounted for 32–47 % of WSOC. Secondary organic carbon (SOC) dominated both the non-fossil and fossil derived WSOC, highlighting the importance of secondary formation to WSOC in severe winter haze episodes. Contributions from fossil emissions to SOC were 61 ± 4 and 50 ± 9 % in Shanghai and Beijing, respectively, significantly larger than those in Guangzhou (36 ± 9 %) and Xi'an (26 ± 9 %). The most important primary sources were biomass burning emissions, contributing 17–26 % of WSOC. The remaining primary sources such as coal combustion, cooking and traffic were generally very small but not negligible contributors, as coal combustion contribution could exceed 10 %. Taken together

with earlier ¹⁴C source apportionment studies in urban, rural, semi-urban and background regions in Asia, Europe and the USA, we demonstrated a dominant contribution of non-fossil emissions (i.e., 75 ± 11 %) to WSOC aerosols in the Northern Hemisphere; however, the fossil fraction is substantially larger in aerosols from East Asia and the eastern Asian pollution outflow, especially during winter, due to increasing coal combustion. Inclusion of our findings can improve a modelling of effects of WSOC aerosols on climate, atmospheric chemistry and public health.

1 Introduction

Water-soluble organic carbon (WSOC) is a large fraction of atmospheric organic aerosols (OA), which contributes approximately 10 to 80 % of the total mass of organic carbon (OC) in aerosols from urban, rural and remote sites (Zappoli et al., 1999; Weber et al., 2007; Ruellan and Cachier, 2001; Wozniak et al., 2012; Mayol-Bracero et al., 2002).

Only 10 to 20 % of total mass of WSOC has been resolved at a molecular level, and it consists of a large variety of chemical species such as mono- and di-carboxylic acids, carbohydrate derivatives, alcohols, aliphatic and aromatic acids and amino acids (Fu et al., 2015; Noziere et al., 2015). Recent studies suggest that the water-soluble fraction of humic like substances (HULIS) is a major component of WSOC, which exhibits light-absorbing properties (Limbeck et al., 2005; Andreae and Gelencser, 2006; Laskin et al., 2015). Therefore, WSOC has significant influences on the Earth's climate either directly by scattering and absorbing radiation or indirectly by altering the hygroscopic properties of aerosols and increasing cloud condensation nuclei (CCN) activity (Asa-Awuku et al., 2011; Cheng et al., 2011; Hecobian et al., 2010).

WSOC can be directly emitted as primary particles mainly from biomass burning emissions or produced from secondary organic aerosol (SOA) formation (Sannigrahi et al., 2006; Kondo et al., 2007; Weber et al., 2007; Bozzetti et al., 2017a, b). Ambient studies provide evidence that SOA formation through the oxidation of volatile organic compounds (VOCs) and gas to particle conversion processes may be a prevalent source of WSOC (Kondo et al., 2007; Weber et al., 2007; Miyazaki et al., 2006; Hecobian et al., 2010). WSOC is therefore thought to be a good proxy for secondary organic carbon (SOC) in the absence of biomass burning (Weber et al., 2007). By contrast, water insoluble OC (WIOC) is thought to be mainly from primary origins with a substantial contribution from fossil fuel emissions (Miyazaki et al., 2006; Zhang et al., 2014a).

Due to a large variety of sources and unresolved formation processes of WSOC, their relative fossil and non-fossil contributions are still poorly constrained. Radiocarbon (^{14}C) analysis of sub-fractions of organic aerosols such as OC, WIOC and WSOC enable an unambiguous, precise and quantitative determination of their fossil and non-fossil sources (Zhang et al., 2012, 2014a, b; Zong et al., 2016; Cao et al., 2017). Meanwhile, the application of aerosol mass spectrometer measurement, positive matrix factorization and multi-linear engine 2 (ME-2) can quantitatively classify organic aerosols into two major types such as hydrocarbon-like OA (HOA) from primary fossil fuel combustion and oxygenated organic aerosol (OOA) from secondary origin (Zhang et al., 2007; Jimenez et al., 2009). Field campaigns with the aerosol mass spectrometer (AMS) have revealed a predominance of OOA in various atmospheric environments, although their sources remain poorly characterized (Zhang et al., 2007; Jimenez et al., 2009). Previous studies found OOA is strongly correlated with WSOC from urban aerosols in Tokyo, Japan, the Pearl River Delta (PRD) in South China and Helsinki, Finland, indicating similar chemical characteristics, sources and formation processes of OOA and WSOC (Kondo et al., 2007; Xiao et al., 2011; Timonen et al., 2013). Similarly, HOA is mostly water insoluble and the major portion of water insoluble OC (WIOC) can

be assigned as HOA (Kondo et al., 2007; Daellenbach et al., 2016). Therefore, ^{14}C measurement of WIOC and WSOC aerosols may provide new insights into sources and formation processes of primary and secondary OA, respectively, which also will elucidate the origin of HOA and OOA as measured by AMS (Zotter et al., 2014b; Zhang et al., 2017).

In this paper, we apply a newly developed method to measure ^{14}C in WSOC of $\text{PM}_{2.5}$ (particulate matter with an aerodynamic diameter of smaller than $2.5\ \mu\text{m}$) samples collected at four Chinese megacities during an extremely severe haze episode in winter 2013 (Y. L. Zhang et al., 2015; Huang et al., 2014). In conjunction with our previous dataset from the same campaign, we quantify fossil and non-fossil emissions from primary and secondary sources of WSOC and WIOC. The dataset is also complemented by previous ^{14}C -based source apportionment studies conducted in urban, rural and remote regions in the Northern Hemisphere to gain an overall picture of the sources of WSOC aerosols.

2 Materials and methods

2.1 Sampling

During January 2013, extremely high concentrations of 24 h $\text{PM}_{2.5}$ (i.e. often $>100\ \mu\text{g m}^{-3}$) were identified in several large cities in eastern China (Huang et al., 2014; Y. L. Zhang et al., 2015). To investigate sources and formation mechanisms of the haze particles, an intensive field campaign was carried out in four large cities, Beijing, Xi'an, Shanghai and Guangzhou, which are representative cities of the Beijing–Tianjin–Hebei region, central-northwestern region, Yangtze Delta Region, and Pearl River Delta Region, respectively. The sampling procedures have been previously described in detail elsewhere (Y. L. Zhang et al., 2015). Briefly, $\text{PM}_{2.5}$ samples were collected on pre-baked ($450\ ^\circ\text{C}$ for 6 h) quartz filters using high-volume samplers for 24 h at a flow rate of $\sim 1.05\ \text{m}^3\ \text{min}^{-1}$ from 5 to 25 January 2013. The sampling sites in each city were located at campuses of universities or at research institutes, at least 100 m away from major emission sources (e.g., roadways, industry and domestic sources). One field blank sample for each site was collected and analyzed. The results reported here were corrected for these field blanks (Zotter et al., 2014a; Cao et al., 2013). All samples were stored at $-20\ ^\circ\text{C}$ before analysis. The $\text{PM}_{2.5}$ mass was gravimetrically measured with an analytical microbalance before and after sampling with the same conditions ($\sim 12\ \text{h}$).

2.2 OC and EC mass determinations

A $1.0\ \text{cm}^2$ filter punches were used for OC and EC mass determination with a OC/EC analyzer (Model4L) using the EUSAAR_2 protocol (Cavalli et al., 2010). The replicate analysis ($n=6$) showed analytical precision with relative standard deviations smaller than 5, 10, and 5 % for OC, EC and TC, respectively. The field blank of OC was on average

$2.0 \pm 1.0 \mu\text{g cm}^{-2}$ (equivalent to $\sim 0.5 \mu\text{g m}^{-3}$), which was used for blank correction for OC. EC data were not corrected for field blank, because such a blank was not detectable.

2.3 Offline-AMS measurement and PMF source apportionment

The water-soluble extracts from the same samples were analyzed by a high-resolution time of flight aerosol mass spectrometer (HR-ToF-AMS) and the resulting mass spectra were used as an inputs for positive matrix factorization (PMF) for the source apportionment of the WSOC, OC and $\text{PM}_{2.5}$. The methodology applied and the AMS-PMF results obtained are detailed in Huang et al. (2014) and will be only briefly described in the following. Here, only data relative to WSOC are used.

Filter punches (the equivalent of $\sim 4 \text{ cm}^2$) were sonicated in 10 mL ultrapure water ($18.2 \text{ M}\Omega \text{ cm}$ at 25°C , $\text{TOC} < 3 \text{ ppb}$) for 20 min at 30°C . The water extracts were aerosolized and the resulting particles were dried with a silica gel diffusion dryer before analysis by the HR-ToF-AMS. For each measurement ten mass spectra were recorded (AMS V-mode, m/z 12–500), with a collection time for each spectrum of 1 min.

Online AMS measurements provide quantitative mass spectra of submicron non-refractory aerosol species, including organic aerosol and ammonium nitrate and sulfate. However, the offline AMS measurements described herein cannot be directly related to ambient concentrations due to uncertainties in nebulization and AMS lens cut-off. Here, we have scaled the organic aerosol mass spectra to water soluble organic aerosol concentrations (WSOM), obtained as WSOC times OM/OC ratios. The latter were determined by the high-resolution analysis of the organic aerosol mass spectra, acquired by the AMS.

The quantitative WSOM mass spectra are used together with other aerosol species (listed below), collectively referred to as “species” hereafter, as PMF inputs. PMF solves the bilinear matrix equation as follows:

$$\mathbf{X}_{ij} = \sum_k \mathbf{G}_{i,k} \mathbf{F}_{k,j} + \mathbf{E}_{i,j}, \quad (1)$$

by following a weighted least squares approach. In the equation, i represent the time index, j a species and k the factor number. \mathbf{X}_{ij} is the input matrix, $\mathbf{G}_{i,k}$ is the matrix of the factor time series, $\mathbf{F}_{k,j}$ is the matrix of the factor profiles and $\mathbf{E}_{i,j}$ the model residual matrix. PMF determines $\mathbf{G}_{i,k}$ and $\mathbf{F}_{k,j}$ such that the ratio of the Frobenius norm of $\mathbf{E}_{i,j}$ over the uncertainty matrix, $\mathbf{s}_{i,j}$, used as model input is minimized.

The species considered as inputs include the quantitative WSOM mass spectra, organic markers (3 anhydrous sugars, 4 lignin breakdown products, 2 resin acids, 4 hopanes, 19 polycyclic aromatic hydrocarbons and their oxygenated derivatives), EC, major ions (Cl^- , NO_3^- , SO_4^{2-} , oxalate, methylsulfonic acid, Na^+ , K^+ , Mg^{2+} , Ca^{2+} , and NH_4^+) and

residual PM. The latter is the difference between total $\text{PM}_{2.5}$ mass and the measured species. It represents our best estimate of the particulate chemical species not measured here, most likely dominated by crustal material.

The Source Finder toolkit (SoFi v.4.9) (Canonaco et al., 2013) from the IGOR Pro software package (Wavemetrics, Inc., Portland, OR, USA) was used to run the PMF algorithm. The PMF was solved by the Multilinear Engine 2 (ME-2, Paatero, 1999), which allows the constraining of the $\mathbf{F}_{k,j}$ elements to vary within a certain range defined by the scalar α ($0 \leq \alpha \leq 1$), such that the modelled $\mathbf{F}'_{k,j}$ equals the following:

$$\mathbf{F}'_{k,j} = \mathbf{F}_{k,j} \pm \alpha \cdot \mathbf{F}_{k,j}. \quad (2)$$

The elements that were constrained in $\mathbf{F}_{k,j}$ matrix can be found in Huang et al. (2014). The factors extracted by ME-2 were interpreted to be related to primary emissions from traffic (TR), biomass burning (BB), coal burning (CC), cooking emissions (CI) and dust as well as from two secondary aerosol fractions. The contributions of the water soluble organic aerosol related to these different factors were determined by the multiplying their relative abundance in the factor profiles by the respective factor time series. The factors WSOM time series were then divided by the respective OM/OC_k calculated from the high-resolution analysis of the factor mass spectral profile to obtain the WSOC_k time series related to each of the factors. The average OM/OC_k are: 1.25, 1.39, 1.49, 1.55, 2.25 and 2.4 for TR, CI, BB, CB, SOA and dust, respectively. In the following analysis, the mass of WSOC_k related to coal burning and traffic were assigned to the fossil WSOC fraction, while the mass of WSOC_k related to biomass burning and cooking emissions were assigned to the non-fossil WSOC fraction (see Sect. 2.5). Meanwhile, the remaining WSOC fractions are assigned to the secondary factors, which can be from both fossil and non-fossil origins. These were considered collectively and compared to the unassigned fossil and non-fossil WSOC, to retrieve the origins of this remaining fraction (see Sect. 2.5).

2.4 ^{14}C measurement of WSOC

^{14}C content of micro-scale WSOC aerosol samples was measured with a newly developed method (Zhang et al., 2014c). Briefly, a 16 mm-diameter punch of each filter was extracted using 10 mL ultrapure water with low TOC impurity (less than 5 ppb). The water extracts were recovered in the 20 mL PFA vials and were then pre-frozen at -20°C more than 5 h before completely dryness in a freeze dryer (Alpha 2-4 LSC, Christ, Germany) for about 24 to 36 h. The residue was re-dissolved in 50 μL of ultrapure water three times and transferred into 200 μL tin capsules (Elementar, Germany). The concentrated samples were heated in the oven at 55 – 60°C until completely dry before the ^{14}C measurements were taken.

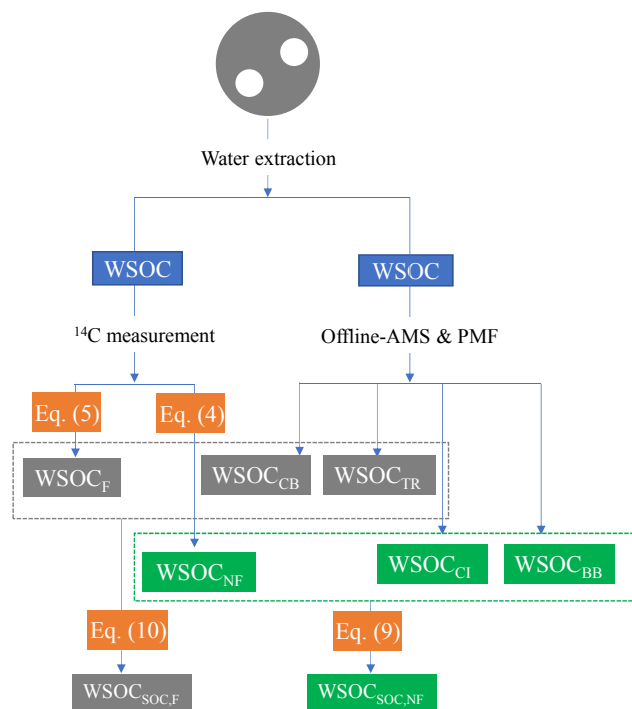


Figure 1. The AMS²-based source apportionment scheme of WSOC aerosols in this study. See text for the equations (i.e., Eqs. 4, 5, 9, 10 in the Sect. 2.5) and the offline AMS & PMF (see the Sect. 2.3).

WSOC extracts in tin capsules were then converted to CO₂ by the oxidation of the carbon-containing samples using an Elemental Analyzer (EA, Model Vario Micro, Elementar, Germany) as a combustion unit (up to 1050 °C). The resulting CO₂ was introduced continuously by a versatile gas inlet system into a gas ion source of the accelerator mass spectrometer MICADAS where ¹⁴C of CO₂ was finally measured (Wacker et al., 2013; Salazar et al., 2015). The ¹⁴C content of OC and EC was measured in our previous study (Y. L. Zhang et al., 2015). ¹⁴C results were expressed as fraction of modern (f_M), i.e., the fraction of the measured ¹⁴C/¹²C ratio related to the ¹⁴C/¹²C ratio of the reference year 1950 (Stuiver, 1977). To correct excess ¹⁴C from nuclear bomb tests in the 1950s and 1960s, f_M values were converted to the fraction of non-fossil (f_{NF}) (Zotter et al., 2014a; Zhang et al., 2012) as follows:

$$f_{NF} = f_M / f_{M,ref}. \quad (3)$$

$f_{M,ref}$ is a reference value of f_M for non-fossil carbon sources including biogenic and biomass burning emissions, which were estimated as 1.08 ± 0.05 (i.e., $f_{M,ref} = (0.5 \times 1.10 + 0.5 \times 1.05)$) (see details in Zhang et al., 2012) for WSOC samples collected in 2013 according to the contemporary atmospheric CO₂ f_M (Levin et al., 2010) and a tree growth model (Mohn et al., 2008).

2.5 AMS²-based source apportionment of WSOC

To better understand the origin of WSOC observed at these sites, WSOC sources were apportioned into several major sources by a combination of ¹⁴C and PMF source apportionments (see Fig. 1). Here, two “AMS” (i.e., accelerator mass spectrometer and aerosol mass spectrometer), such a combined approach was named “AMS²-based source apportionment”.

WSOC concentration from non-fossil (WSOC_{NF}) and fossil (WSOC_F) sources were calculated as follows:

$$\text{WSOC}_{NF} = \text{WSOC} \cdot f_{NF}(\text{WSOC}) \quad (4)$$

$$\text{WSOC}_F = \text{WSOC} - \text{WSOC}_{NF}. \quad (5)$$

The mass concentration of WSOC was derived from the subtraction of TC mass measured from a water-extracted filter from that measured with an un-treated filter (Zhang et al., 2012):

$$\text{WSOC} = \text{TC}_{\text{un-treated}} - \text{TC}_{\text{water-extracted}}. \quad (6)$$

Based on mass balance, WIOC concentrations from non-fossil (WIOC_{NF}) and fossil (WIOC_F) sources were calculated as follows:

$$\text{WIOC}_{NF} = \text{OC}_{NF} - \text{WSOC}_{NF} \quad (7)$$

$$\text{WIOC}_F = \text{OC}_F - \text{WSOC}_F, \quad (8)$$

where OC concentrations from non-fossil (OC_{NF}) and fossil (OC_F) sources were obtained by mass and ¹⁴C measurement of the OC fraction, which were reported previously (Y. L. Zhang et al., 2015).

The non-fossil and fossil fuel derived WSOC can be apportioned into primary and secondary OC:

$$\text{WSOC}_{NF} = \text{WSOC}_{\text{POC},NF} + \text{WSOC}_{\text{SOC},NF} \quad (9)$$

$$\text{WSOC}_F = \text{WSOC}_{\text{POC},F} + \text{WSOC}_{\text{SOC},F}. \quad (10)$$

WSOC_{POC,NF} can be sub-divided into the following three major primary emissions including cooking emission (WSOC_{CI}) and biomass burning (WSOC_{BB}).

$$\text{WSOC}_{\text{POC},NF} = \text{WSOC}_{CI} + \text{WSOC}_{BB}. \quad (11)$$

Similarly, WSOC_{POC,F} can be sub-divided into the following two major primary emissions including traffic (WSOC_{TR}) and coal combustion (WSOC_{CB}).

$$\text{WSOC}_{\text{POC},F} = \text{WSOC}_{TR} + \text{WSOC}_{CB}, \quad (12)$$

where primary fractions such as WSOC_{CI}, WSOC_{BB}, WSOC_{TR} and WSOC_{CB} are previously estimated by the offline AMS–PMF approach (Huang et al., 2014; Daellenbach et al., 2016; Bozzetti et al., 2017a, b).

An uncertainty propagation scheme using a Latin-hypercube sampling (LHS) model was implemented to properly estimate overall uncertainties, including measurement

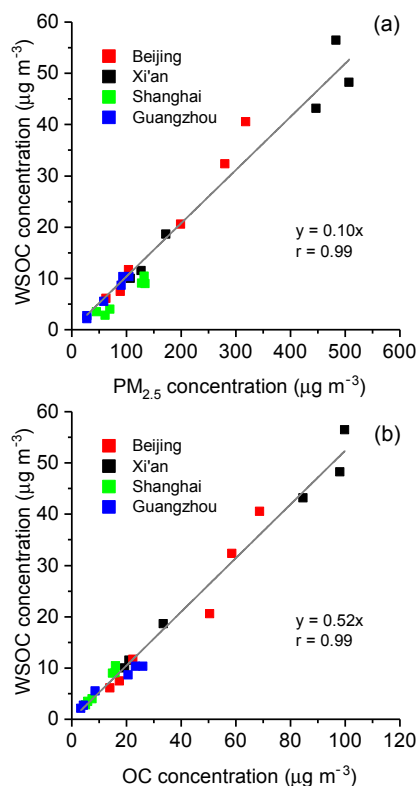


Figure 2. Linear relationships ($p < 0.01$) of WSOC with $\text{PM}_{2.5}$ (a) and OC concentrations (b).

uncertainties of the mass determinations of carbon species (i.e., OC, EC, TC, WSOC, WIOC) and ^{14}C measurement, blank corrections from field blanks, and estimation of $f_{\text{M,ref}}$ (Y. L. Zhang et al., 2015).

3 Results and discussion

3.1 Overall results

During the haze periods of January 2013, the highest daily average $\text{PM}_{2.5}$ concentrations were found in Xi'an ($345 \mu\text{g m}^{-3}$) followed by Beijing ($158 \mu\text{g m}^{-3}$), Shanghai ($90 \mu\text{g m}^{-3}$) and Guangzhou ($68 \mu\text{g m}^{-3}$). These levels were much higher than the China's national ambient air quality standards (i.e., $35 \mu\text{g m}^{-3}$). Indeed, several studies have already reported the chemical composition, source and formation mechanism of $\text{PM}_{2.5}$ in many large cities during the haze events of January 2013 in eastern China. For examples, Huang et al. (2014) revealed that the secondary aerosol formation contributed to 44–71 % of OA in Beijing, Xi'an, Shanghai, and Guangzhou during this extremely haze event in China (Huang et al., 2014). By ^{14}C -based source apportionment conducted in the same campaign, Zhang et al. (2015) have reported that carbonaceous aerosol pollution was driven to a large (often dominant) extent by SOA formation from

both fossil and biomass-burning sources (Y. L. Zhang et al., 2015). For all four cities, the 24 h average levels of WSOC were significantly correlated with the levels of $\text{PM}_{2.5}$ and OC ($R = 0.99$, $p < 0.01$, Fig. 2), suggesting that WSOC and OA may have similar sources and formation processes and thus have important implications for OC loadings and associated environmental and health effects. However, the sources of WSOC remain poorly constrained. In this study, we measured the ^{14}C content of WSOC aerosols in six samples (three with the highest, three with average PM mass) for each city to report on heavily and moderately polluted days (HPD and MPD, respectively) (Y. L. Zhang et al., 2015). The ^{14}C contents of OC and EC of the same samples were reported previously (Y. L. Zhang et al., 2015).

WSOC on average accounted for $53 \pm 8.0\%$ (ranging from 40–65 %) of OC including all samples from the four sites, which was consistent with previous estimates. Based on these measurements, the concentrations of WSOC from non-fossil sources (WSOC_{NF}) spanned from 1.41 to $45.3 \mu\text{g m}^{-3}$ with a mean of $10.6 \pm 12.1 \mu\text{g m}^{-3}$, whereas the corresponding range for WSOC from fossil fuel emissions (WSOC_{F}) was 0.44 to $20.1 \mu\text{g m}^{-3}$ with a mean of $5.3 \pm 4.9 \mu\text{g m}^{-3}$ (Fig. 3). Similar to $\text{PM}_{2.5}$ levels, the highest concentrations of WSOC_{NF} and WSOC_{F} were observed in northern China in Xi'an and Beijing (Xi'an > Beijing), followed by the two southern sites of Shanghai and Guangzhou. Non-fossil contributions (mean \pm standard deviation) to total WSOC were 53 ± 5 , 75 ± 4 , 48 ± 2 and $68 \pm 6\%$ in Beijing, Xi'an, Shanghai, and Guangzhou, respectively. Thus, fossil contributions were notably higher in Beijing and Shanghai than in Xi'an and Guangzhou. Such a trend was also observed for OC (Y. L. Zhang et al., 2015), suggesting relatively high contribution from fossil fuel emissions to OC and WSOC due to large coal usage. Despite these fossil emissions, non-fossil sources were important or even dominant contributors for all the studied sites, which may be associated with primary and secondary OA from regional and local biomass burning emissions. As shown in Fig. 4, non-fossil WSOC was significantly correlated with levoglucosan, indicating that a large fraction of non-fossil WSOC was indeed from biomass burning emissions. In addition, no significant (or only a negative) correlation (Fig. 4) was found between levoglucosan and fraction of fossil to WSOC, suggesting that fossil fuel source is very unlikely to be a major or important contributor of levoglucosan even in the regions (e.g., Xi'an and Beijing in this study) where coal combustion is important during the cold period (Y.-L. Zhang et al., 2015). It should also be noted that formation of SOA derived from biogenic VOCs may also have contributed to WSOC_{NF} in Guangzhou, where temperatures during the sampling period were significantly higher (i.e., $5\text{--}18^\circ\text{C}$) than those in other cities (i.e., -12 to $+9^\circ\text{C}$) (Bozzetti et al., 2017b). Although both fossil and non-fossil WSOC concentrations were dramatically enhanced during HPD compared to those during MPD, their relative contributions did not change significantly in Beijing and Shang-

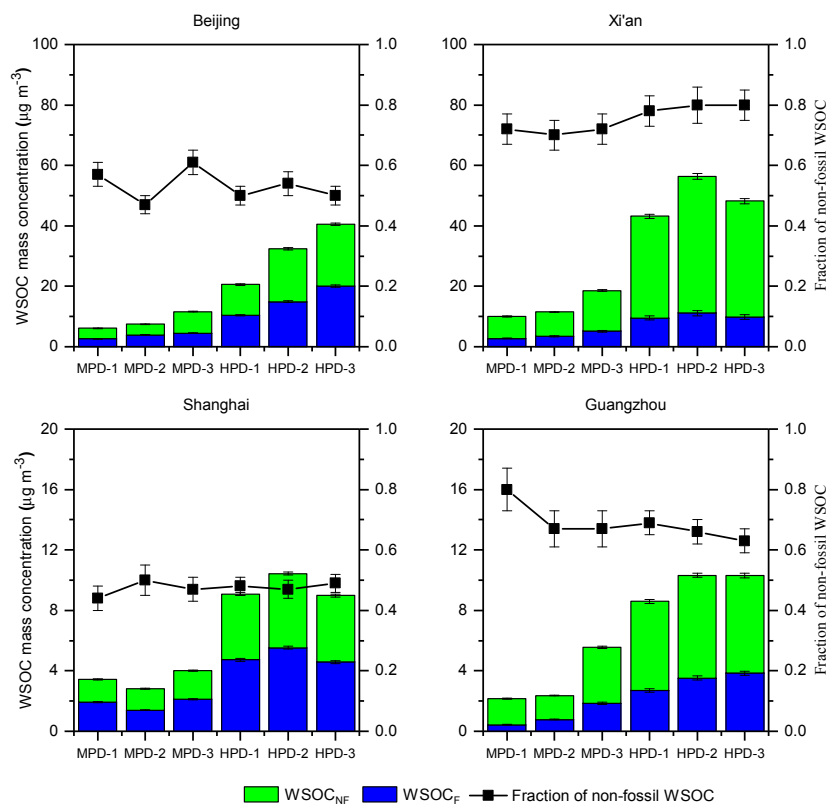


Figure 3. Mass concentrations ($\mu\text{g m}^{-3}$) of WSOC from non-fossil and fossil fuel sources (WSOC_{NF} and WSOC_{F} , respectively) as well as non-fossil fractions of the WSOC aerosols from Beijing, Xi'an, Shanghai and Guangzhou during moderately polluted days (MPD) and heavily polluted days (HPD). Note the different scaling for different cities.

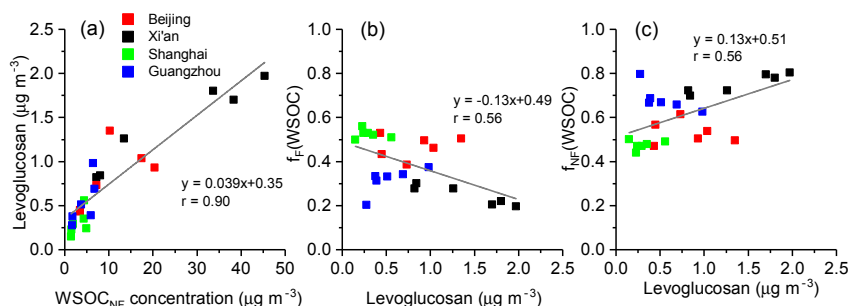


Figure 4. Relationships of non-fossil derived WSOC (WSOC_{NF}) and levoglucosan (a), levoglucosan and the fraction of fossil in WSOC ($f_{\text{F}}(\text{WSOC})$) (b) and levoglucosan and the fraction of non-fossil in WSOC ($f_{\text{NF}}(\text{WSOC})$) (c).

hai, whereas a small increasing and decreasing trend in the non-fossil fraction was found in Xi'an and Guangzhou, respectively (Fig. 3). This suggests that the source pattern of WSOC in Beijing and Shanghai remained similar between HPD and MPD, but the increase in the WSOC concentrations was rather enhanced by additional fossil fuel and biogenic (or biomass) burning emissions in Guangzhou and Xi'an, respectively. It should be noted that the meteorological conditions played significant roles in the haze formation in eastern China during winter 2013, and has already been well docu-

mented (R. Zhang et al., 2014). However, the details sources of WSOC and WIOC were still unclear.

3.2 WSOC versus WIOC

To compare sources of WSOC and WIOC aerosols, the mass concentrations and ^{14}C contents of WIOC were also derived based on mass balance. The ^{14}C -based source apportionment of WIOC and the relationship between $f_{\text{NF}}(\text{WSOC})$ and $f_{\text{NF}}(\text{WIOC})$ are presented in Figs. 5 and 6a, respec-

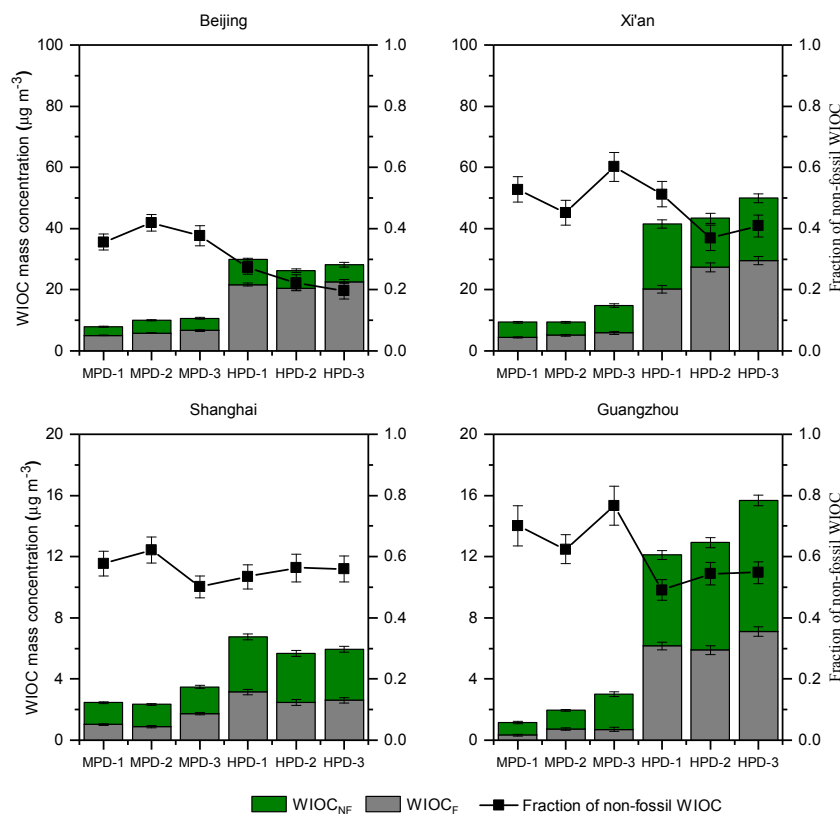


Figure 5. Mass concentrations ($\mu\text{g m}^{-3}$) of WIOC from non-fossil and fossil fuel sources (WIOC_{NF} and WIOC_F, respectively) as well as non-fossil fractions in the WIOC aerosols from Beijing, Xi'an, Shanghai and Guangzhou during moderately polluted days (MPD) and heavily polluted days (HPD). Note the different scaling for different cities.

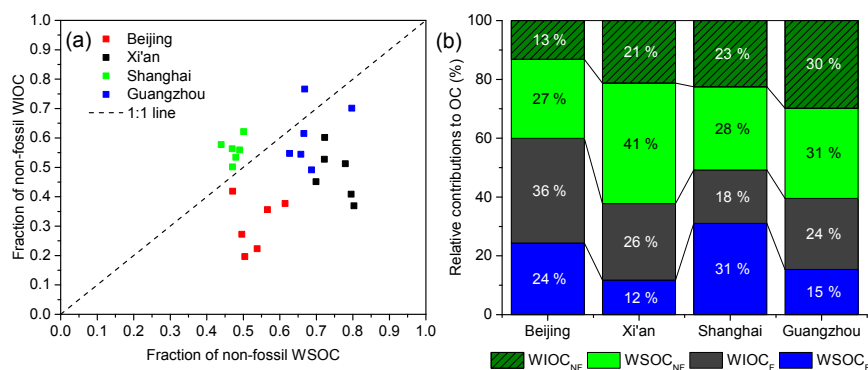


Figure 6. Relationship between the fraction of non-fossil WIOC and WSOC (a) and averaged relative contribution (%) to OC from WSOC and WIOC from non-fossil and fossil sources (b).

tively. It shows that non-fossil contributions to WSOC were larger than those of WIOC for nearly all samples in Beijing, Xi'an and Guangzhou. On average, the majority (60–70 %) of the fossil OC was water insoluble at these three sites (see Fig. 6b), indicating that fossil-derived OA mostly consisted of hydrophobic components and thus is less water soluble than OA from non-fossil sources. This result is consistent with findings reported elsewhere such as at an urban

or rural site in Switzerland (Zhang et al., 2013), a remote site on Hainan Island, southern China (Zhang et al., 2014a) and at two rural sites on the east coast of the United States (Wozniak et al., 2012). Meanwhile, the fossil OC in Shanghai, the dominant fraction of OC, was more water soluble (Fig. 6b), suggesting an enhanced SOA formation from fossil VOCs from vehicle emissions and/or coal burning in this city. As shown in Figure 6b, non-fossil OA was enriched in

Table 1. Compilation of literature values of relative fossil fuel contributions (fossil %) to the WSOC aerosols in East/South Asia, USA and Europe.

Site	Location	Season	Size	WSOC ($\mu\text{g m}^{-3}$)	WSOC/OC	Fossil %	References
East Asia							
Urban	Beijing, China	Winter/2013	PM _{2.5}	19.8	0.49	47	This work
Urban	Xi'an, China	Winter 2013	PM _{2.5}	31.3	0.53	25	This work
Urban	Shanghai, China	Winter 2013	PM _{2.5}	6.5	0.58	52	This work
Urban	Guangzhou, China	Winter 2013	PM _{2.5}	6.6	0.53	32	This work
Urban	Beijing, China	Winter 2014	PM _{2.5}	14.7	0.40	56	Fang et al. (2017)
Urban	Beijing, China	Winter 2011	PM _{4.3}	15	0.50	55	Zhang et al. (2014b)
Urban	Beijing, China	Winter 2013	PM _{2.5}	9.3	0.31	54	Yan et al. (2017)
Urban	Guangzhou, China	Winter 2012/2013	PM _{2.5}	4.1	0.38	33	Liu et al. (2014)
Urban	Guangzhou, China	Winter 2011	PM ₁₀	4.5	0.43	28.5	Zhang et al. (2014b)
Urban	Xi'an, China	Autumn 2009	PM _{2.5}	5.1	0.28	31	Pavuluri et al. (2013)
Urban	Xi'an, China	Autumn 2010	TSP	8.1	0.28	29	Pavuluri et al. (2013)
Urban	Wuhan, China	Winter 2013	PM _{2.5}	13.7	0.45	37	Liu et al. (2016)
Urban	Sapporo, Japan	Summer/Autumn 2010	PM ₃	1	0.43	15	Pavuluri et al. (2013)
Urban	Sapporo, Japan	Summer 2011	TSP	1.1	0.24	12	Pavuluri et al. (2013)
Urban	Sapporo, Japan	Spring 2010	TSP	1.1	0.31	11	Pavuluri et al. (2013)
Urban	Sapporo, Japan	Autumn 2011	TSP	1.8	0.48	18.3	Pavuluri et al. (2013)
Urban	Sapporo, Japan	Winter 2010	TSP	0.9	0.45	40.2	Pavuluri et al. (2013)
Background	Jeju Island, Korea	Winter 2014	PM _{2.5}	2.2	0.66	50	Fang et al. (2017)
Background	Jeju Island, Korea	Spring 2011	PM _{2.5}	2.0		37.5	Kirillova et al. (2014a)
Background	Jeju Island, Korea	Spring 2011	TSP	3.0		25	Kirillova et al. (2014a)
Average						33 ± 14	
South Asia							
Background	Hainan, China	Annual 2005/2006	PM _{2.5}	3.9	0.54	18	Zhang et al. (2014b)
Background	Hainan, China	Winter 2005/2006	PM _{2.5}	6.2	0.57	14.5	Zhang et al. (2014b)
Background	Hainan, China	Summer 2005/2006	PM _{2.5}	1.4	0.40	17.7	Zhang et al. (2014b)
Background	Hanimaadhoo, Maldives	Annual 2008/2009	TSP	0.5		17	Kirillova et al. (2013)
Background	Sinhagad, India	Annual 2008/2009	TSP	3.0		24	Kirillova et al. (2013)
Background	Hanimaadhoo, Maldives	Spring 2012	PM _{2.5}	0.6	0.62	14	Bosch et al. (2014)
Urban	Delhi, India	Winter 2010/2011	PM _{2.5}	22.0		21	Kirillova et al. (2014b)
Average						18 ± 4	
Europe and USA							
Urban	Gothenburg, Sweden	Winter 2005	PM _{2.5}	1.1	0.48	23	Szidat et al. (2009)
Urban	Gothenburg, Sweden	Summer 2006	PM _{2.5}	0.8	0.61	30	Szidat et al. (2009)
Rural	Gothenburg, Sweden	Winter 2005		1.2	0.53	27	Szidat et al. (2009)
Rural/semi-urban	Stockholm, Sweden	Summer 2009	TSP			12	Kirillova et al. (2010)
Urban	Zürich, Switzerland	Summer 2002	PM ₁₀	2.1	0.54	14	Szidat et al. (2004)
Urban	Zürich, Switzerland	Winter 2008	PM ₁₀	2.8	0.60	26.8	Zhang et al. (2013)
Urban	Moleno, Switzerland	Summer 2006	PM ₁₀	5.3	0.67	30	Zhang et al. (2013)
Urban	Bern, Switzerland	Winter 2009	PM ₁₀		0.39	14	Zhang et al. (2014b)
Urban	Atlanta, USA	Summer 2004	PM _{2.5}	2.3	0.59	26.5	Weber et al. (2007)
Rural	Millbrook, USA	Annual 2006/2007	TSP		0.36	12	Wozniak et al. (2012)
Rural	Harcum, USA	Annual 2006/2007	TSP		0.38	14	Wozniak et al. (2012)
Regional background	Cesar, Netherlands	Annual 2011/2012	PM _{2.5}	2.3	0.65	21	Dusek et al. (2017)
Average						21 ± 8	

water-soluble fractions (i.e., $60 \pm 8\%$) for all cities, associated with the hydrophilic properties of biogenic-derived SOA and biomass-burning derived primary organic aerosol (POA) and SOA, which are composed of a large fraction of polar and highly oxygenated compounds (Mayol-Bracero et al., 2002; Sullivan et al., 2011; Noziere et al., 2015). Thus, non-fossil OC has more water-soluble components than fossil OC does. It should be noted that relative contributions of WSOC_{NF} and WSOC_F are similar in Beijing and Shanghai, whereas WSOC_{NF} is much higher than WSOC_F in Xi'an and

Guangzhou. This suggests larger contribution of non-fossil sources to WSOC aerosols in Xi'an and Guangzhou than those in Beijing and Shanghai.

3.3 High contribution of secondary formation to WSOC

WSOC was further apportioned into fossil sources such as coal burning (CB), traffic (TR) and SOC (SOC,F) as well as non-fossil sources such as biomass burning (BB), cook-

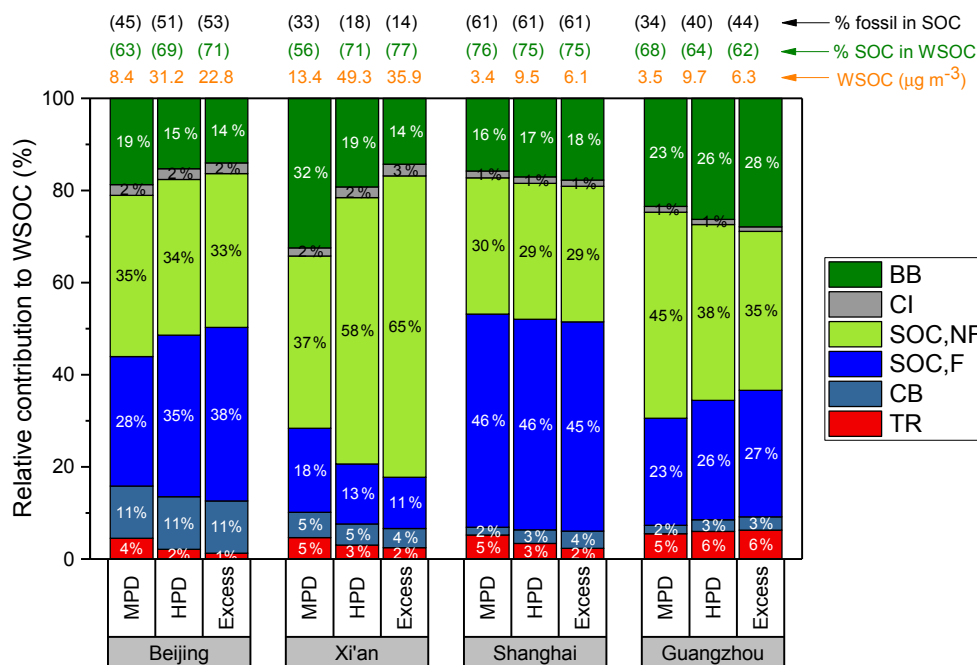


Figure 7. Relative contributions (%) to WSOC from biomass burning, as well as secondary organic carbon (SOC) from fossil and non-fossil sources ($\text{WSOC}_{\text{SOC,F}}$ and $\text{WSOC}_{\text{SOC,NF}}$, respectively) in different cities during moderately polluted days (MPD) and heavily polluted days (HPD), as well as their corresponding excess (Excess = HPD-MPD). The numbers above the bars refer to the average WSOC concentrations and the SOC fractions (%) of WSOC.

ing (CI) and SOC (SOC_{NF}) using a AMS^2 based source apportionment (see Sect. 2.5 and Fig. 1). SOC dominated WSOC during both the HPD and MPD with a mean contribution of $67 \pm 9\%$, highlighting the importance of SOC formation to the WSOC aerosols in winter pollution events. This is consistent with our previous findings for total $\text{PM}_{2.5}$ mass and bulk carbonaceous aerosols (i.e., total carbon, sum of OC and EC) (Huang et al., 2014; Y. L. Zhang et al., 2015). The increase in SOC contribution to WSOC during HPD compared to MPD can be largely due to fossil contribution in Beijing but non-fossil emissions in Xi'an. In Shanghai and Guangzhou, the source pattern of WSOC was not significantly different between MPD and HPD. Fossil contributions to WSOC_{SOC} were $50 \pm 9\%$ in Beijing, $61 \pm 4\%$ in Shanghai, associated with SOA from local and transported fossil fuel derived precursors at these sites (Guo et al., 2014). This contribution drops to 36 ± 9 and $26 \pm 9\%$ in Guangzhou and Xi'an, respectively, due to higher biomass-burning contribution to SOC. Despite of the general importance of fossil SOC, formation of non-fossil WSOC_{SOC} becomes especially relevant during HPD especially in Xi'an (Fig. 7), which may be explained by competing effects in SOC formation from fossil versus non-fossil precursors. It can be hypothesized for extremely polluted episodes that more hydrophilic volatile compounds that were emitted from biomass burning precursors preferentially form SOC compounds via heterogeneous reaction or processing of dust particles, compared to

highly hydrophobic precursors from fossil sources, a point that should be subjected to future laboratory and field experiments. The most important primary sources of WSOC were biomass burning emissions, and their contributions were higher in Xi'an ($26 \pm 7\%$) and Guangzhou ($25 \pm 6\%$) than those found in Beijing ($17 \pm 6\%$) and Shanghai ($17 \pm 5\%$). The remaining primary sources such as coal combustion, cooking and traffic were generally very small contributors of WSOC due to lower water solubility, although coal combustion could exceed 10% in Beijing. It should be noted that WSOC was dominated by SOC formation with a mean contribution of 61 ± 10 and $72 \pm 12\%$ (average for all four cities) to non-fossil and fossil fuel derived WSOC, respectively.

4 Summary and implications

Our study demonstrates that non-fossil emissions are generally a dominant contributor of WSOC aerosols during extreme haze events in representative major cities of China, which is in agreement with WSOC source information identified in aerosols with different size fractions (e.g., TSP, PM_{10} and $\text{PM}_{2.5}$) observed in the Northern Hemisphere at urban, rural, semi-urban, and background sites in East/South Asia, Europe and USA (Table 1). The ^{14}C -based source apportionment database shows a mean non-fossil fraction of $73 \pm 11\%$ across all sites. This overwhelming non-fossil contribution to WSOC is consistently observed throughout the year, which is

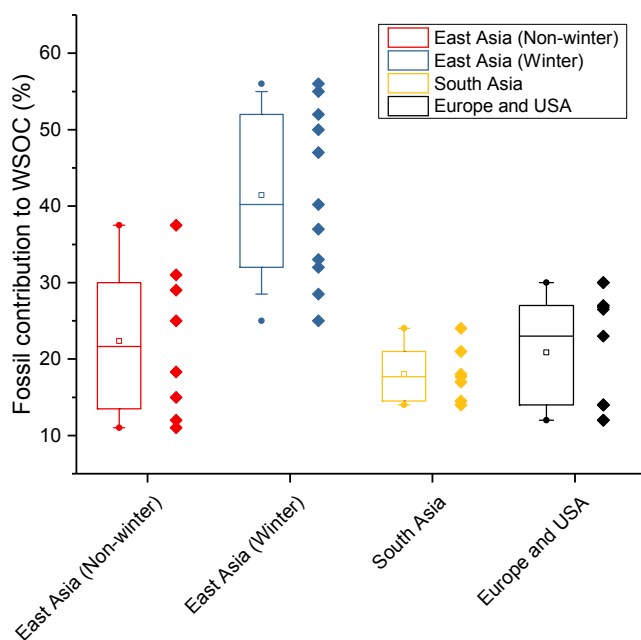


Figure 8. Box-plot of the fossil contribution (%) to the WSOC aerosols in East Asia, South Asia, the USA and Europe. The box represents the 25th (lower line), 50th (middle line) and 75th (top line) percentiles; the empty square within the box represent the mean values; the end lines of the vertical bars represent the 10th (below the box) and 90th (above the box) percentiles; the solid dots represent the maximum and minimum values; the solid diamonds represent the individual data (Table 1). The data from East Asia is grouped by winter and non-winter seasons.

associated with seasonally dependent biomass burning emissions and/or biogenic-derived SOC formation. Our study provides evidence that the presence of oxidized OA, which is to a large extent water soluble, in the Northern Hemisphere (Zhang et al., 2007) is mainly derived from biogenic derived SOA and/or biomass burning sources. The overall importance of non-fossil emissions to the WSOC aerosols results from large contributions of SOC formation from biogenic precursors (e.g., most likely during summer) and relatively high water-solubility of primary biomass burning particles (e.g., most likely during winter) compared to those emitted from fossil fuel emissions such as coal combustion and vehicle exhaust. Despite the importance of non-fossil sources, a significant fossil fraction is also observed in the WSOC aerosols from polluted regions in East Asia and sites influenced by East Asian continental outflow (Table 1, Fig. 8). This fossil contribution is apparently higher than in this region than in the USA and Europe, which is due to large industrial and residential coal usage as well as vehicle emissions. From our observation, the increases in the fossil fractions of WSOC were mostly from SOC formation. Since WSOC has hygroscopic properties, our findings suggest that SOC formation from non-fossil emissions have significant implications

on aerosol-induced climate effects. In addition, fossil-derived SOC formation may also become important in polluted regions with large amounts of fossil fuel emissions, such as in China and other emerging countries. Low combustion efficiencies and consequently high emission factors in most of the combustion processes in China may further be responsible for increased concentrations of fossil precursors which may be oxidized to form water-soluble SOA in the atmosphere and contribute substantially to the WSOC aerosols. The enhanced WSOC levels may also originate from aging of fossil POA during the long-range transport of aerosols (Kirillova et al., 2014a). It is also interesting to note that fossil contribution during winter in East Asia is generally higher than those in the rest of the year, although a relatively large fossil fraction could be occasionally found as well. Such seasonal dependence was not observed in other regions, suggesting the importance of fossil contribution to WSOC due to increasing coal combustions during winter in China. This study provides a more detailed source apportionment of WSOC, which could improve modelling of climate and health effects as well as the understanding of atmospheric chemistry of WSOC in the polluted atmosphere such as China and provide a scientific basis for policy decisions on air pollution emissions mitigation.

Data availability. All data needed to evaluate the conclusions in the paper are present in the paper. Additional data related to this paper may be requested from the authors (Yan-Lin Zhang, zhangyanlin@nuist.edu.cn).

Author contributions. YLZ, SS, RJH, JJC and ASHP designed the study. YLZ and GS perform ^{14}C measurement. YLZ and SS interpreted the ^{14}C data. RJH, IEH, CB and KD performed the offline AMS analysis and interpret the data. YLZ and IEH perform ^{14}C -AMS-PMF source apportionments. YLZ wrote the paper. All authors reviewed and commented on the paper.

Competing interests. The authors declare that they have no conflict of interest.

Special issue statement. This article is part of the special issue “Multiphase chemistry of secondary aerosol formation under severe haze”. It does not belong to a conference.

Acknowledgements. This work was supported by The National Key Research and Development Program of China (Grant No. 2017YFC0212704), the National Natural Science Foundation of China (Grant Nos. 41603104 and 91644103) and the Priority Academic Program Development of Jiangsu Higher Education Institutions (grant PAPD).

Edited by: Daniel Knopf

Reviewed by: two anonymous referees

References

- Andreae, M. O. and Gelencsér, A.: Black carbon or brown carbon? The nature of light-absorbing carbonaceous aerosols, *Atmos. Chem. Phys.*, 6, 3131–3148, <https://doi.org/10.5194/acp-6-3131-2006>, 2006.
- Asa-Awuku, A., Moore, R. H., Nenes, A., Bahreini, R., Holloway, J. S., Brock, C. A., Middlebrook, A. M., Ryerson, T. B., Jimenez, J. L., DeCarlo, P. F., Hecobian, A., Weber, R. J., Stickel, R., Tanner, D. J., and Huey, L. G.: Airborne cloud condensation nuclei measurements during the 2006 Texas Air Quality Study, *J. Geophys. Res.*, 116, D11201, <https://doi.org/10.1029/2010jd014874>, 2011.
- Bosch, C., Andersson, A., Kirillova, E. N., Budhavant, K., Tiwari, S., Praveen, P. S., Russell, L. M., Beres, N. D., Ramanathan, V., and Gustafsson, O.: Source-diagnostic dual-isotope composition and optical properties of water-soluble organic carbon and elemental carbon in the South Asian outflow intercepted over the Indian Ocean, *J. Geophys. Res.*, 119, 11743–11759, <https://doi.org/10.1002/2014JD022127>, 2014.
- Bozzetti, C., El Haddad, I., Salameh, D., Daellenbach, K. R., Fermo, P., Gonzalez, R., Minguillón, M. C., Iinuma, Y., Poulain, L., Elser, M., Müller, E., Slowik, J. G., Jaffrezo, J. L., Baltensperger, U., Marchand, N., and Prévôt, A. S. H.: Organic aerosol source apportionment by offline-AMS over a full year in Marseille, *Atmos. Chem. Phys.*, 17, 8247–8268, <https://doi.org/10.5194/acp-17-8247-2017>, 2017a.
- Bozzetti, C., Sosedova, Y., Xiao, M., Daellenbach, K. R., Ulevicius, V., Dudoitis, V., Mordas, G., Byčenkienė, S., Plauškaitė, K., Vlachou, A., Golly, B., Chazeau, B., Besombes, J. L., Baltensperger, U., Jaffrezo, J. L., Slowik, J. G., El Haddad, I., and Prévôt, A. S. H.: Argon offline-AMS source apportionment of organic aerosol over yearly cycles for an urban, rural, and marine site in northern Europe, *Atmos. Chem. Phys.*, 17, 117–141, <https://doi.org/10.5194/acp-17-117-2017>, 2017b.
- Canonaco, F., Crippa, M., Slowik, J. G., Baltensperger, U., and Prévôt, A. S. H.: SoFi, an IGOR-based interface for the efficient use of the generalized multilinear engine (ME-2) for the source apportionment: ME-2 application to aerosol mass spectrometer data, *Atmos. Meas. Tech.*, 6, 3649–3661, <https://doi.org/10.5194/amt-6-3649-2013>, 2013.
- Cao, F., Zhang, Y.-L., Szidat, S., Zapf, A., Wacker, L., and Schwiowski, M.: Microgram-level radiocarbon determination of carbonaceous particles in firn and ice samples: pretreatment and OC/EC separation, *Radiocarbon*, 55, 383–390, 2013.
- Cao, F., Zhang, Y., Ren, L., Liu, J., Li, J., Zhang, G., Liu, D., Sun, Y., Wang, Z., Shi, Z., and Fu, P.: New insights into the sources and formation of carbonaceous aerosols in China: potential applications of dual-carbon isotopes, *Nat. Sci. Rev.*, 4, 804–806, <https://doi.org/10.1093/nsr/nwx097>, 2017.
- Cavalli, F., Viana, M., Yttri, K. E., Genberg, J., and Putaud, J.-P.: Toward a standardised thermal-optical protocol for measuring atmospheric organic and elemental carbon: the EUSAAR protocol, *Atmos. Meas. Tech.*, 3, 79–89, <https://doi.org/10.5194/amt-3-79-2010>, 2010.
- Cheng, Y., He, K. B., Zheng, M., Duan, F. K., Du, Z. Y., Ma, Y. L., Tan, J. H., Yang, F. M., Liu, J. M., Zhang, X. L., Weber, R. J., Bergin, M. H., and Russell, A. G.: Mass absorption efficiency of elemental carbon and water-soluble organic carbon in Beijing, China, *Atmos. Chem. Phys.*, 11, 11497–11510, <https://doi.org/10.5194/acp-11-11497-2011>, 2011.
- Daellenbach, K. R., Bozzetti, C., Krepelova, A. K., Canonaco, F., Wolf, R., Zotter, P., Fermo, P., Crippa, M., Slowik, J. G., Sosedova, Y., Zhang, Y., Huang, R. J., Poulain, L., Szidat, S., Baltensperger, U., El Haddad, I., and Prevot, A. S. H.: Characterization and source apportionment of organic aerosol using offline aerosol mass spectrometry, *Atmos. Meas. Tech.*, 9, 23–39, <https://doi.org/10.5194/amt-9-23-2016>, 2016.
- Dusek, U., Hitzemberger, R., Kasper-Giebl, A., Kistler, M., Meijer, H. A. J., Szidat, S., Wacker, L., Holzinger, R., and Röckmann, T.: Sources and formation mechanisms of carbonaceous aerosol at a regional background site in the Netherlands: insights from a year-long radiocarbon study, *Atmos. Chem. Phys.*, 17, 3233–3251, <https://doi.org/10.5194/acp-17-3233-2017>, 2017.
- Fang, W., Andersson, A., Zheng, M., Lee, M., Holmstrand, H., Kim, S.-W., Du, K., and Gustafsson, Ö.: Divergent Evolution of Carbonaceous Aerosols during Dispersal of East Asian Haze, *Scientific Reports*, 7, 10422, <https://doi.org/10.1038/s41598-017-10766-4>, 2017.
- Fu, P., Kawamura, K., Chen, J., Qin, M., Ren, L., Sun, Y., Wang, Z., Barrie, L. A., Tachibana, E., Ding, A., and Yamashita, Y.: Fluorescent water-soluble organic aerosols in the High Arctic atmosphere, *Sci. Rep.*, 5, 9845, <https://doi.org/10.1038/srep09845>, 2015.
- Guo, S., Hu, M., Zamora, M. L., Peng, J., Shang, D., Zheng, J., Du, Z., Wu, Z., Shao, M., Zeng, L., Molina, M. J., and Zhang, R.: Elucidating severe urban haze formation in China, *P. Natl. Acad. Sci. USA*, 111, 17373–17378, <https://doi.org/10.1073/pnas.1419604111>, 2014.
- Hecobian, A., Zhang, X., Zheng, M., Frank, N., Edgerton, E. S., and Weber, R. J.: Water-Soluble Organic Aerosol material and the light-absorption characteristics of aqueous extracts measured over the Southeastern United States, *Atmos. Chem. Phys.*, 10, 5965–5977, <https://doi.org/10.5194/acp-10-5965-2010>, 2010.
- Huang, R. J., Zhang, Y., Bozzetti, C., Ho, K. F., Cao, J. J., Han, Y., Daellenbach, K. R., Slowik, J. G., Platt, S. M., Canonaco, F., Zotter, P., Wolf, R., Pieber, S. M., Bruns, E. A., Crippa, M., Ciarelli, G., Piazzalunga, A., Schwikowski, M., Abbaszade, G., Schnelle-Kreis, J., Zimmermann, R., An, Z., Szidat, S., Baltensperger, U., El Haddad, I., and Prevot, A. S.: High secondary aerosol contribution to particulate pollution during haze events in China, *Nature*, 514, 218–222, <https://doi.org/10.1038/nature13774>, 2014.
- Jimenez, J. L., Canagaratna, M. R., Donahue, N. M., Prevot, A. S. H., Zhang, Q., Kroll, J. H., DeCarlo, P. F., Allan, J. D., Coe, H., Ng, N. L., Aiken, A. C., Docherty, K. S., Ulbrich, I. M., Grieshop, A. P., Robinson, A. L., Duplissy, J., Smith, J. D., Wilson, K. R., Lanz, V. A., Hueglin, C., Sun, Y. L., Tian, J., Laaksonen, A., Raatikainen, T., Rautiainen, J., Vaattovaara, P., Ehn, M., Kulmala, M., Tomlinson, J. M., Collins, D. R., Cubison, M. J., Dunlea, E. J., Huffman, J. A., Onasch, T. B., Alfarra, M. R., Williams, P. I., Bower, K., Kondo, Y., Schneider, J., Drewnick, F., Borrmann, S., Weimer, S., Demerjian, K., Salcedo, D., Cottrell, L., Griffin, R., Takami, A., Miyoshi, T., Hatakeyama, S., Shimono, A., Sun, J. Y., Zhang, Y. M., Dzepina,

- K., Kimmel, J. R., Sueper, D., Jayne, J. T., Herndon, S. C., Trimborn, A. M., Williams, L. R., Wood, E. C., Middlebrook, A. M., Kolb, C. E., Baltensperger, U., and Worsnop, D. R.: Evolution of organic aerosols in the atmosphere, *Science*, 326, 1525–1529, <https://doi.org/10.1126/science.1180353>, 2009.
- Kirillova, E. N., Sheesley, R. J., Andersson, A., and Gustafsson, O.: Natural abundance ^{13}C and ^{14}C analysis of water-soluble organic carbon in atmospheric aerosols, *Anal. Chem.*, 82, 7973–7978, <https://doi.org/10.1021/AC1014436>, 2010.
- Kirillova, E. N., Andersson, A., Sheesley, R. J., Kruså, M., Praveen, P. S., Budhavant, K., Safai, P. D., Rao, P. S. P., and Gustafsson, Ö.: ^{13}C and ^{14}C -based study of sources and atmospheric processing of water-soluble organic carbon (WSOC) in South Asian aerosols, *J. Geophys. Res.*, 118, 614–626, <https://doi.org/10.1002/jgrd.50130>, 2013.
- Kirillova, E. N., Andersson, A., Han, J., Lee, M., and Gustafsson, O.: Sources and light absorption of water-soluble organic carbon aerosols in the outflow from northern China, *Atmos. Chem. Phys.*, 14, 1413–1422, <https://doi.org/10.5194/acp-14-1413-2014>, 2014a.
- Kirillova, E. N., Andersson, A., Tiwari, S., Srivastava, A. K., Bisht, D. S., and Gustafsson, O.: Water-soluble organic carbon aerosols during a full New Delhi winter: Isotope-based source apportionment and optical properties, *J. Geophys. Res.*, 119, 3476–3485, <https://doi.org/10.1002/2013jd020041>, 2014b.
- Kondo, Y., Miyazaki, Y., Takegawa, N., Miyakawa, T., Weber, R. J., Jimenez, J. L., Zhang, Q., and Worsnop, D. R.: Oxygenated and water-soluble organic aerosols in Tokyo, *J. Geophys. Res.*, 112, D01203, <https://doi.org/10.1029/2006jd007056>, 2007.
- Laskin, A., Laskin, J., and Nizkorodov, S. A.: Chemistry of Atmospheric Brown Carbon, *Chem. Rev. (Washington, DC, U. S.)*, 115, 4335–4382, <https://doi.org/10.1021/cr5006167>, 2015.
- Levin, I., Naegler, T., Kromer, B., Diehl, M., Francey, R. J., Gomez-Pelaez, A. J., Steele, L. P., Wagenbach, D., Weller, R., and Worthy, D. E.: Observations and modelling of the global distribution and long-term trend of atmospheric $^{14}\text{CO}_2$, *Tellus B*, 62, 26–46, <https://doi.org/10.1111/j.1600-0889.2009.00446.x>, 2010.
- Limbeck, A., Handler, M., Neuberger, B., Klatzer, B., and Puxbaum, H.: Carbon-specific analysis of humic-like substances in atmospheric aerosol and precipitation samples, *Anal. Chem.*, 77, 7288–7293, <https://doi.org/10.1021/ac0509531>, 2005.
- Liu, J., Li, J., Vonwiller, M., Liu, D., Cheng, H., Shen, K., Salazar, G., Agrios, K., Zhang, Y., He, Q., Ding, X., Zhong, G., Wang, X., Szidat, S., and Zhang, G.: The importance of non-fossil sources in carbonaceous aerosols in a megacity of central China during the 2013 winter haze episode: A source apportionment constrained by radiocarbon and organic tracers, *Atmos. Environ.*, 144, 60–68, <https://doi.org/10.1016/j.atmosenv.2016.08.068>, 2016.
- Liu, J. W., Li, J., Zhang, Y. L., Liu, D., Ding, P., Shen, C. D., Shen, K. J., He, Q. F., Ding, X., Wang, X. M., Chen, D. H., Szidat, S., and Zhang, G.: Source Apportionment Using Radiocarbon and Organic Tracers for $\text{PM}_{2.5}$ Carbonaceous Aerosols in Guangzhou, South China: Contrasting Local- and Regional-Scale Haze Events, *Environ. Sci. Technol.*, 48, 12002–12011, <https://doi.org/10.1021/Es503102w>, 2014.
- Mayol-Bracero, O. L., Guyon, P., Graham, B., Roberts, G., Andreae, M. O., Decesari, S., Facchini, M. C., Fuzzi, S., and Artaxo, P.: Water-soluble organic compounds in biomass burning aerosols over Amazonia – 2. Apportionment of the chemical composition and importance of the polyacidic fraction, *J. Geophys. Res.*, 107, D8091, <https://doi.org/10.1029/2001jd000522>, 2002.
- Miyazaki, Y., Kondo, Y., Takegawa, N., Komazaki, Y., Fukuda, M., Kawamura, K., Mochida, M., Okuzawa, K., and Weber, R. J.: Time-resolved measurements of water-soluble organic carbon in Tokyo, *J. Geophys. Res.*, 111, D23206, <https://doi.org/10.1029/2006JD007125>, 2006.
- Mohn, J., Szidat, S., Fellner, J., Rechberger, H., Quartier, R., Buchmann, B., and Emmenegger, L.: Determination of biogenic and fossil CO_2 emitted by waste incineration based on $^{14}\text{CO}_2$ and mass balances, *Bioresour. Technol.*, 99, 6471–6479, <https://doi.org/10.1016/j.biortech.2007.11.042>, 2008.
- Noziere, B., Kalberer, M., Claeys, M., Allan, J., D’Anna, B., Decesari, S., Finessi, E., Glasius, M., Grgic, I., Hamilton, J. F., Hoffmann, T., Iinuma, Y., Jaoui, M., Kahnt, A., Kampf, C. J., Kourtchev, I., Maenhaut, W., Marsden, N., Saarikoski, S., Schnelle-Kreis, J., Surratt, J. D., Szidat, S., Szmigielski, R., and Wisthaler, A.: The molecular identification of organic compounds in the atmosphere: state of the art and challenges, *Chem. Rev.*, 115, 3919–3983, <https://doi.org/10.1021/cr5003485>, 2015.
- Pavuluri, C. M., Kawamura, K., Uchida, M., Kondo, M., and Fu, P. Q.: Enhanced modern carbon and biogenic organic tracers in Northeast Asian aerosols during spring/summer, *J. Geophys. Res.*, 118, 2362–2371, <https://doi.org/10.1002/Jgrd.50244>, 2013.
- Ruellan, S. and Cachier, H.: Characterisation of fresh particulate vehicular exhausts near a Paris high flow road, *Atmos. Environ.*, 35, 453–468, [https://doi.org/10.1016/S1352-2310\(00\)00110-2](https://doi.org/10.1016/S1352-2310(00)00110-2), 2001.
- Salazar, G., Zhang, Y. L., Agrios, K., and Szidat, S.: Development of a method for fast and automatic radiocarbon measurement of aerosol samples by online coupling of an elemental analyzer with a MICADAS AMS, *Nucl. Instr. Meth. Phys. Res. B.*, 361, 163–167, <https://doi.org/10.1016/j.nimb.2015.03.051>, 2015.
- Sannigrahi, P., Sullivan, A. P., Weber, R. J., and Ingall, E. D.: Characterization of water-soluble organic carbon in urban atmospheric aerosols using solid-state C-13 NMR spectroscopy, *Environ. Sci. Technol.*, 40, 666–672, <https://doi.org/10.1021/Es051150i>, 2006.
- Stuiver, M.: Discussion: Reporting of ^{14}C data, *Radiocarbon*, 19, 355–363, 1977.
- Sullivan, A. P., Frank, N., Kenski, D. M., and Collett, J. L.: Application of high-performance anion-exchange chromatography-pulsed amperometric detection for measuring carbohydrates in routine daily filter samples collected by a national network: 2. Examination of sugar alcohols/polyols, sugars, and anhydro-sugars in the upper Midwest, *J. Geophys. Res.*, 116, D08303, <https://doi.org/10.1029/2010jd014169>, 2011.
- Szidat, S., Jenk, T. M., Gäggeler, H. W., Synal, H. A., Fisseha, R., Baltensperger, U., Kalberer, M., Samburova, V., Wacker, L., Saurer, M., Schwikowski, M., and Hajdas, I.: Source apportionment of aerosols by ^{14}C measurements in different carbonaceous particle fractions, *Radiocarbon*, 46, 475–484, 2004.
- Szidat, S., Ruff, M., Perron, N., Wacker, L., Synal, H.-A., Hallquist, M., Shannigrahi, A. S., Yttri, K. E., Dye, C., and Simpson, D.: Fossil and non-fossil sources of organic carbon (OC) and elemental carbon (EC) in Göteborg, Sweden, *Atmos. Chem. Phys.*, 9, 1521–1535, <https://doi.org/10.5194/acp-9-1521-2009>, 2009.

- Timonen, H., Carbone, S., Aurela, M., Saarnio, K., Saarikoski, S., Ng, N. L., Canagaratna, M. R., Kulmala, M., Kerminen, V. M., Worsnop, D. R., and Hillamo, R.: Characteristics, sources and water-solubility of ambient submicron organic aerosol in springtime in Helsinki, Finland, *J. Aerosol Sci.*, 56, 61–77, <https://doi.org/10.1016/j.jaerosci.2012.06.005>, 2013.
- Wacker, L., Fahrni, S. M., Hajdas, I., Molnar, M., Synal, H. A., Szidat, S., and Zhang, Y. L.: A versatile gas interface for routine radiocarbon analysis with a gas ion source, *Nucl. Instrum. Meth. B*, 294, 315–319, <https://doi.org/10.1016/j.nimb.2012.02.009>, 2013.
- Weber, R. J., Sullivan, A. P., Peltier, R. E., Russell, A., Yan, B., Zheng, M., de Gouw, J., Warneke, C., Brock, C., Holloway, J. S., Atlas, E. L., and Edgerton, E.: A study of secondary organic aerosol formation in the anthropogenic-influenced southeastern United States, *J. Geophys. Res.*, 112, D13302, <https://doi.org/10.1029/2007jd008408>, 2007.
- Wozniak, A. S., Bauer, J. E., and Dickhut, R. M.: Characteristics of water-soluble organic carbon associated with aerosol particles in the eastern United States, *Atmos. Environ.*, 46, 181–188, <https://doi.org/10.1016/j.atmosenv.2011.10.001>, 2012.
- Xiao, R., Takegawa, N., Zheng, M., Kondo, Y., Miyazaki, Y., Miyakawa, T., Hu, M., Shao, M., Zeng, L., Gong, Y., Lu, K., Deng, Z., Zhao, Y., and Zhang, Y. H.: Characterization and source apportionment of submicron aerosol with aerosol mass spectrometer during the PRIDE-PRD 2006 campaign, *Atmos. Chem. Phys.*, 11, 6911–6929, <https://doi.org/10.5194/acp-11-6911-2011>, 2011.
- Yan, C., Zheng, M., Bosch, C., Andersson, A., Desyaterik, Y., Sullivan, A. P., Collett, J. L., Zhao, B., Wang, S., He, K., and Gustafsson, O.: Important fossil source contribution to brown carbon in Beijing during winter, *Sci. Rep.*, 7, 43182, <https://doi.org/10.1038/srep43182>, 2017.
- Zappoli, S., Andracchio, A., Fuzzi, S., Facchini, M. C., Gelencser, A., Kiss, G., Krivacsy, Z., Molnar, A., Meszaros, E., Hansson, H. C., Rosman, K., and Zebuhr, Y.: Inorganic, organic and macromolecular components of fine aerosol in different areas of Europe in relation to their water solubility, *Atmos. Environ.*, 33, 2733–2743, [https://doi.org/10.1016/S1352-2310\(98\)00362-8](https://doi.org/10.1016/S1352-2310(98)00362-8), 1999.
- Zhang, Q., Jimenez, J. L., Canagaratna, M. R., Allan, J. D., Coe, H., Ulbrich, I., Alfarra, M. R., Takami, A., Middlebrook, A. M., Sun, Y. L., Dzepina, K., Dunlea, E., Docherty, K., DeCarlo, P. F., Salcedo, D., Onasch, T., Jayne, J. T., Miyoshi, T., Shimojo, A., Hatakeyama, S., Takegawa, N., Kondo, Y., Schneider, J., Drewnick, F., Borrmann, S., Weimer, S., Demerjian, K., Williams, P., Bower, K., Bahreini, R., Cottrell, L., Griffin, R. J., Rautiainen, J., Sun, J. Y., Zhang, Y. M., and Worsnop, D. R.: Ubiquity and dominance of oxygenated species in organic aerosols in anthropogenically-influenced Northern Hemisphere midlatitudes, *Geophys. Res. Lett.*, 34, L13801, <https://doi.org/10.1029/2007gl029979>, 2007.
- Zhang, R., Li, Q., and Zhang, R.: Meteorological conditions for the persistent severe fog and haze event over eastern China in January 2013, *Sci. China Earth Sci.*, 57, 26–35, <https://doi.org/10.1007/s11430-013-4774-3>, 2014.
- Zhang, Y., Ren, H., Sun, Y., Cao, F., Chang, Y., Liu, S., Lee, X., Agrios, K., Kawamura, K., Liu, D., Ren, L., Du, W., Wang, Z., Prevot, A. S. H., Szidat, S., and Fu, P.: High Contribution of Nonfossil Sources to Submicrometer Organic Aerosols in Beijing, China, *Environ. Sci. Technol.*, 51, 7842–7852, <https://doi.org/10.1021/acs.est.7b01517>, 2017.
- Zhang, Y. L., Perron, N., Ciobanu, V. G., Zotter, P., Minguilón, M. C., Wacker, L., Prévôt, A. S. H., Baltensperger, U., and Szidat, S.: On the isolation of OC and EC and the optimal strategy of radiocarbon-based source apportionment of carbonaceous aerosols, *Atmos. Chem. Phys.*, 12, 10841–10856, <https://doi.org/10.5194/acp-12-10841-2012>, 2012.
- Zhang, Y. L., Zotter, P., Perron, N., Prévôt, A. S. H., Wacker, L., and Szidat, S.: Fossil and non-fossil sources of different carbonaceous fractions in fine and coarse particles by radiocarbon measurement, *Radiocarbon*, 55, 1510–1520, 2013.
- Zhang, Y. L., Huang, R. J., El Haddad, I., Ho, K. F., Cao, J. J., Han, Y., Zotter, P., Bozzetti, C., Daellenbach, K. R., Canonaco, F., Slowik, J. G., Salazar, G., Schwikowski, M., Schnelle-Kreis, J., Abbaszade, G., Zimmermann, R., Baltensperger, U., Prévôt, A. S. H., and Szidat, S.: Fossil vs. non-fossil sources of fine carbonaceous aerosols in four Chinese cities during the extreme winter haze episode of 2013, *Atmos. Chem. Phys.*, 15, 1299–1312, <https://doi.org/10.5194/acp-15-1299-2015>, 2015.
- Zhang, Y.-L., Li, J., Zhang, G., Zotter, P., Huang, R.-J., Tang, J.-H., Wacker, L., Prévôt, A. S. H., and Szidat, S.: Radiocarbon-based source apportionment of carbonaceous aerosols at a regional background site on hainan Island, South China, *Environ. Sci. Technol.*, 48, 2651–2659, <https://doi.org/10.1021/es4050852>, 2014a.
- Zhang, Y.-L., Liu, J.-W., Salazar, G. A., Li, J., Zotter, P., Zhang, G., Shen, R.-r., Schäfer, K., Schnelle-Kreis, J., Prévôt, A. S. H., and Szidat, S.: Micro-scale (μg) radiocarbon analysis of water-soluble organic carbon in aerosol samples, *Atmos. Environ.*, 97, 1–5, <https://doi.org/10.1016/j.atmosenv.2014.07.059>, 2014b.
- Zhang, Y.-L., Schnelle-Kreis, J. r., Abbaszade, G. I., Zimmermann, R., Zotter, P., Shen, R.-R., Schafer, K., Shao, L., Prévôt, A. S. H., and Szidat, S. N.: Source apportionment of elemental carbon in Beijing, China: Insights from radiocarbon and organic marker measurements, *Environ. Sci. Technol.*, 49, 8408–8415, 2015.
- Zong, Z., Wang, X., Tian, C., Chen, Y., Han, G., Li, J., and Zhang, G.: Source and formation characteristics of water-soluble organic carbon in the anthropogenic-influenced Yellow River Delta, North China, *Atmos. Environ.*, 144, 124–132, <https://doi.org/10.1016/j.atmosenv.2016.08.078>, 2016.
- Zotter, P., Ciobanu, V. G., Zhang, Y. L., El-Haddad, I., Macchia, M., Daellenbach, K. R., Salazar, G. A., Huang, R. J., Wacker, L., Hueglin, C., Piazzalunga, A., Fermo, P., Schwikowski, M., Baltensperger, U., Szidat, S., and Prévôt, A. S. H.: Radiocarbon analysis of elemental and organic carbon in Switzerland during winter-smog episodes from 2008 to 2012 – Part I: Source apportionment and spatial variability, *Atmos. Chem. Phys.*, 14, 13551–13570, <https://doi.org/10.5194/acp-14-13551-2014>, 2014a.
- Zotter, P., El-Haddad, I., Zhang, Y., Hayes, P. L., Zhang, X., Lin, Y.-H., Wacker, L., Schnelle-Kreis, J., Abbaszade, G., Zimmermann, R., Surratt, J. D., Weber, R., Jimenez, J. L., Szidat, S., Baltensperger, U., and Prévôt, A. S. H.: Diurnal cycle of fossil and nonfossil carbon using radiocarbon analyses during CalNex, *J. Geophys. Res.*, 119, 6818–6835, <https://doi.org/10.1002/2013jd021114>, 2014b.